NAVAL AIR WARFARE CENTER AIRCRAFT DIVISION
PATUXENT RIVER, MARYLAND

TECHNICAL REPORT

REPORT NO: NAWCADPAX/TR-2007/5

ELEVATED-TEMPERATURE LIFE LIMITING BEHAVIOR OF HI-NICALON SiC/SiC CERAMIC MATRIX COMPOSITE IN INTERLAMINAR SHEAR

by

Sung R. Choi
Robert W. Kowalik
Donald J. Alexander
Narottam P. Bansal

2 March 2007

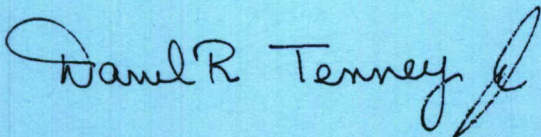Approved for public release; distribution is unlimited.

ELEVATED-TEMPERATURE LIFE LIMITING BEHAVIOR OF HI-NICALON SiC/SiC CERAMIC MATRIX COMPOSITE IN INTERLAMINAR SHEAR

by

Sung R. Choi
Robert W. Kowalik
Donald J. Alexander
Naval Air Systems Command, Patuxent River, MD 20670

N. P. Bansal
National Aeronautics and Space Administration
Glenn Research Center, Cleveland, OH 44135

RELEASED BY:

Darrel R Tenney   2 Mar 2007
_____
DARREL TENNEY / AIR-4.3.4.1 / DATE
Head, Metals and Ceramics Branch
Naval Air Warfare Center Aircraft Division

NAWCADPAX/TR-2007/5

REPORT DOCUMENTATION PAGE		Form Approved OMB No. 0704-0188

Public reporting burden for this collection of information is estimated to average 1 hour per response, including the time for reviewing instructions, searching existing data sources, gathering and maintaining the data needed, and completing and reviewing this collection of information. Send comments regarding this burden estimate or any other aspect of this collection of information, including suggestions for reducing this burden, to Department of Defense, Washington Headquarters Services, Directorate for Information Operations and Reports (0704-0188), 1215 Jefferson Davis Highway, Suite 1204, Arlington, VA 22202-4302. Respondents should be aware that notwithstanding any other provision of law, no person shall be subject to any penalty for failing to comply with a collection of information if it does not display a currently valid OMB control number. **PLEASE DO NOT RETURN YOUR FORM TO THE ABOVE ADDRESS.**

1. REPORT DATE	2. REPORT TYPE	3. DATES COVERED
2 March 2007	Technical Report	FY06

4. TITLE AND SUBTITLE	5a. CONTRACT NUMBER
Elevated-Temperature Life Limiting Behavior of Hi-Nicalon SiC/SiC Ceramic Matrix Composite in Interlaminar Shear	5b. GRANT NUMBER
	5c. PROGRAM ELEMENT NUMBER

6. AUTHOR(S)	5d. PROJECT NUMBER
Sung R. Choi	
Robert W. Kowalik	5e. TASK NUMBER
Donald J. Alexander	
Narottam P. Bansal	5f. WORK UNIT NUMBER

7. PERFORMING ORGANIZATION NAME(S) AND ADDRESS(ES)	8. PERFORMING ORGANIZATION REPORT NUMBER
Naval Air Warfare Center Aircraft Division 22347 Cedar Point Road, Unit #6 Patuxent River, Maryland 20670-1161	NAWCADPAX/TR-2007/5

9. SPONSORING/MONITORING AGENCY NAME(S) AND ADDRESS(ES)	10. SPONSOR/MONITOR'S ACRONYM(S)
Naval Air Systems Command 47123 Buse Road Unit IPT Patuxent River, Maryland 20670-1547	11. SPONSOR/MONITOR'S REPORT NUMBER(S)

12. DISTRIBUTION/AVAILABILITY STATEMENT

Approved for public release; distribution is unlimited.

13. SUPPLEMENTARY NOTES

14. ABSTRACT

Assessments of life limiting behavior of a gas-turbine grade, melt-infiltrated Hi-Nicalon SiC continuous fiber-reinforced SiC ceramic matrix composite (CMC) were made in interlaminar shear using both stress rupture and constant stress-rate testing at 1316°C in air. The composite exhibited appreciable life limiting behavior with a life susceptibility parameter of n_s=22-24, estimated based on a proposed phenomenological life prediction model together with the experimental data. The phenomenological life model was in good agreement in prediction between the stress rupture and the constants stress-rate data, validating its appropriateness in describing the life limiting phenomenon of the CMC coupons subjected to interlaminar shear. Despite some limitations in material availability, time to failure and shear strength data exhibited a statistical relation, typically observed in Mode I loading for many isotropic brittle solids. The results of this work also indicated that the governing mechanism(s) associated with failure in interlaminar shear remained almost unchanged, regardless of the type of loading configurations, either in stress rupture or in constant stress rate. This additionally indicates that simplistic constant shear stress-rate testing can be used as a possible means of life prediction test methodology for CMCs even in interlaminar shear at elevated temperatures when relatively short lifetimes are expected.

15. SUBJECT TERMS
Ceramic matrix composite (CMC); SiC/SiC composite; interlaminar shear; life limiting behavior; life prediction; mechanical properties

16. SECURITY CLASSIFICATION OF:			17. LIMITATION OF ABSTRACT	18. NUMBER OF PAGES	19a. NAME OF RESPONSIBLE PERSON Sung R. Choi
a. REPORT	b. ABSTRACT	c. THIS PAGE			19b. TELEPHONE NUMBER (include area code); EMAIL
Unclassified	Unclassified	Unclassified	SAR	38	301-342-8009; sung.choi1@navy.mil

Standard Form 298 (Rev. 8-98)
Prescribed by ANSI Std. Z39-18

i

SUMMARY

Assessments of life limiting behavior of a gas-turbine grade, melt-infiltrated Hi-Nicalon SiC continuous fiber-reinforced SiC ceramic matrix composite (CMC) were made in interlaminar shear using both stress rupture and constant stress-rate testing at $1316°C$ in air. The composite exhibited appreciable life limiting behavior with a life susceptibility parameter of n_s=22-24, estimated based on a proposed phenomenological life prediction model together with the experimental data. The phenomenological life model was in good agreement in prediction between the stress rupture and the constants stress-rate data, validating its appropriateness in describing the life limiting phenomenon of the CMC coupons subjected to interlaminar shear. Despite some limitations in material availability, time to failure and shear strength data exhibited a statistical relation, typically observed in Mode I loading for many isotropic brittle solids. The results of this work also indicated that the governing mechanism(s) associated with failure in interlaminar shear remained almost unchanged, regardless of the type of loading configurations, either in stress rupture or in constant stress rate. This additionally indicates that simplistic constant shear stress-rate testing can be used as a possible means of life prediction test methodology for CMCs even in interlaminar shear at elevated temperatures when relatively short lifetimes are expected.

Contents

ACKNOWLEDGEMENTS

1. INTRODUCTION

The successful development and design of continuous fiber-reinforced ceramic matrix composites (CMCs), particularly in aeroengine applications, are dependent on better understanding of their life limiting properties such as fatigue, slow crack growth (SCG), stress rupture, creep, and environmental degradation. Life limiting behavior of CMCs can occur individually or simultaneously combined with some of these properties depending on temperature and environment. Accurate and reliable evaluation of life limiting behavior under specific loading/temperature/environmental conditions is important to ensure accurate life prediction of structural CMC components.

Although fiber-reinforced CMCs have shown much improved resistance to fracture and increased damage tolerance in in-plane direction, as compared with the monolithic ceramics, inherent material/processing defects, voids, and/or cracks in the matrix-rich or fiber-matrix interface regions can still cause delamination under interlaminar normal or shear stress, resulting in loss of stiffness or in some cases structural failure. Interlaminar tensile and shear strength behaviors of CMCs have been characterized in view of their unique interfacial architectures and importance in structural applications [1-4]. It has been reported that many 2-D woven SiC/SiC CMCs exhibited poor interlaminar properties with interlaminar shear strength of 30-50 MPa and interlaminar tensile strength of 10-20 MPa [5].

Most efforts regarding the assessments of life limiting properties of CMCs have been made for the Mode I in-plane direction. Few studies have been done on the issue of life limiting of CMCs in *interlaminar shear* at elevated temperatures. Because of their inherent architectural features, CMCs would exhibit life limiting behavior in interlaminar shear at elevated temperatures. In a previous study [6], the life limiting properties of a cross-plied glass ceramic composite (Hi-Nic SiC fiber-reinforced barium strontium aluminosilicate matrix composite, SiC/BSAS) were evaluated in shear at $1100^{\circ}C$ in air by using double-notch shear (DNS) test specimens subjected to constant shear stress-rate loading. The composite exhibited shear strength degradation with decreasing stress rates, analogous to the SCG process occurring in tension for many ceramics at elevated temperatures. The life limiting susceptibility was significant with a life susceptibility parameter (n) of about 10. The life of the CMC in shear was limited by SCG or damage accumulation/growth. The life limiting behavior in shear was modeled using a power-law type of pseudo-SCG process of a crack located at fiber-matrix interfaces. This model has been applied to other CMCs such as SiC/SiCs, SiC/MAS (magnesium aluminosilicate), and C/SiC but with some statistically limited data [7].

This report, as an extension of the previous work [6,7], describes life limiting behavior of a commercial, gas-turbine grade, melt infiltration (MI) Hi-Nic SiC fiber-reinforced SiC CMC (designated Hi-Nic SiC/SiC) in interlaminar shear. DNS test specimens using a significant sample size were tested at $1316^{\circ}C$ in air under stress rupture loading. Life limiting behavior of the Hi-Nic SiC/SiC composite was analyzed using a power-law type of phenomenological life model proposed previously [6,7]. Additional experimental data, determined in constant shear stress-rate testing at $1316^{\circ}C$ in air, were also used to further validate the proposed model.

Statistical aspects of data, failure mechanism, and life prediction test methodology in shear are also described.

2. EXPERIMENTAL PROCEDURES

2.1 MATERIAL

A 2-D woven Hi-Nicalon™ SiC fiber-reinforced SiC CMC (Hi-Nic SiC/SiC), fabricated by GE Power System Composites (Newark, DL; vintage '02), was used in this study. Detailed descriptions of the composite and its processing can be found elsewhere [8]. Briefly, Hi-Nic SiC fibers, produced in tow, were woven into 2-D, 5 harness-satin cloth at Techni-Weave, Albany, New York. The cloth preforms of the composite were cut into 200 mm x 150 mm, 8 ply-stacked, and chemically vapor infiltrated (CVI) with a thin boron nitride (BN)-based interface coating followed by SiC matrix overcoating. Remaining matrix porosity was filled with SiC particulates and then with molten silicon at 1400°C, a process termed slurry casting and MI. The MI SiC/SiC composite was composed of about 39 vol% fibers, about 8 vol% BN coating, about 25 vol% SiC coating, and about 28 vol% SiC particulates, silicon and pores. The nominal dimensions of the composite panels fabricated were about 200 mm by 150 mm with a thickness of about 2.0 mm. The composite exhibited ~ 300 MPa in-plane tensile strength, 36±3 MPa interlaminar shear strength, 13±1 MPa transthickness tensile strength, 183±7 GPa in-plane elastic modulus (determined by the impulse excitation of vibration technique, ASTM C 1259 [10]), and 2.36±0.02 g/cm³ bulk density, all estimated at ambient temperature [5,10]. A typical micrograph of the cross section of the composite is shown in figure 1. Porosity was evident with some significant voids in tows and matrices which were probably attributed to poor CVI, slurry, and/or MI processes. Porosity was estimated to be approximately 10%.
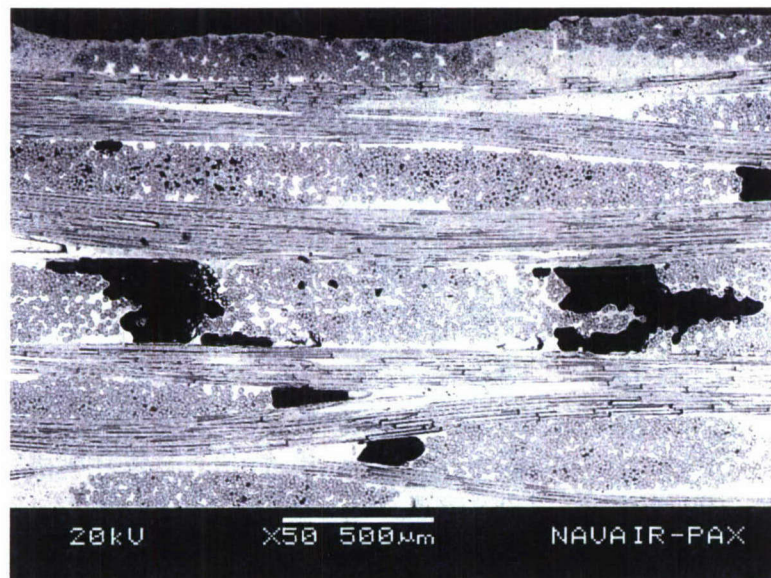

Figure 1: Microstructure of Hi-Nic SiC/SiC CMC used in the current work.

2.2 STRESS RUPTURE TESTING

Stress rupture testing for the Hi-Nic SiC/SiC composite was conducted in interlaminar shear at 1316°C in air. The DNS test specimens were machined from the composite panels. Test specimens were 12.7 mm wide (W) and 30 mm long (L). The thickness of test specimens corresponded to the nominal thickness (=2 mm) of the composite. Two notches, 0.3 mm wide (h) and 6 mm (L_n) away from each other, were made into each test specimen such that the two notches were extended to the middle of the specimen so that shear failure occurred on the plane between the notch tips. Schematics of a DNS test specimen and the test setup are shown in figure 2. Test fixtures were all made of α-SiC. In-situ axial displacement of test specimens was monitored for some selected samples using an LVDT placed between the upper and lower fixtures, incorporated with a data acquisition system. Since test specimens were relatively thin (2 mm) and somewhat irregular in their surfaces due to the nature of 2-D fabrication, a specially designed, tubular type of antibuckling guides was used. Each test specimen was kept prior to testing for about 20 min at 1316°C for thermal equilibration. A total of 22 test specimens was tested over a total of 5 different levels of applied shear stresses ranging from 8 to 17.8 MPa. Test specimen configurations and test procedure were followed in accordance with ASTM C 1425 [11]. All testing was performed using an electromechanical test frame (Model 8562, Instron, Canton, MA). Time to failure of each specimen tested was determined from the data acquisition system. Interlaminar shear stress, i.e., the average nominal shear stress, was calculated using the following relation:

$$\tau = \frac{P}{WL_n} \tag{1}$$

where τ is the applied shear stress, P is the applied load (in compression), and W and L_n are the specimen width and the distance between the two notches, respectively (see figure 2).
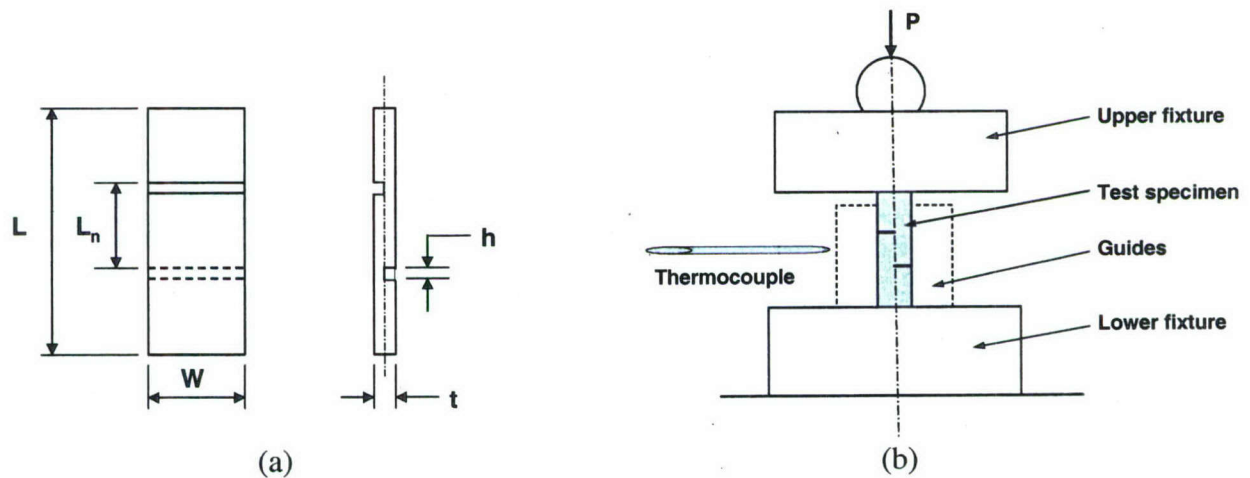

Figure 2: (a) Configurations of DNS test specimen and (b) schematic showing a test setup used in this work.

2.3 CONSTANT SHEAR STRESS-RATE TESTING

Additional interlaminar shear testing was also conducted for the composite using constant shear stress-rate testing. Each test specimen was subjected to a given applied shear stress-rate until it failed. A total of three different shear stress rates ranging from 5 to 0.005 MPa/s was employed with a total of five specimens tested at each applied shear stress rate. One test specimen was tested at 0.0005 MPa/s. Test fixtures, test temperature, test specimen configuration, and test frame were the same as those used in stress rupture testing. This type of testing, in which strength is determined as a function of stress rate, is often called 'constant stress-rate' or 'dynamic fatigue' testing when applied to glasses and monolithic ceramics to determine their SCG behavior in tension or flexure [12,13]. The purpose of this supplementary testing was to determine life limiting behavior in constant stress-rate loading and to compare it with that in stress rupture, with which the phenomenological life prediction model can be validated. Constant shear stress-rate testing at elevated temperatures has been used to determine time-dependent shear failure behavior of some CMCs such as SiC/SiCs, SiC/MAS, C/SiC [7], and SiC/BSAS [6]. Applied shear stress rate ($\dot{\tau}$) was calculated using the relation:

$$\dot{\tau} = \frac{\dot{P}}{WL_n} \tag{2}$$

where $\dot{P}$ is the applied load rate (in compression), which can be applied directly to test specimens via a test frame in load control.

3. RESULTS

3.1 STRESS RUPTURE

All specimens tested in stress rupture at 1316°C failed in typical shear mode along their respective interlaminar shear planes. An example showing such a mode of shear failure is shown in figure 3. The results of stress rupture testing are presented in figure 4, where time to failure is plotted as a function of applied shear stress. The data clearly show an evidence of life limiting behavior, where time to failure decreased with increasing applied shear stress rate. The solid line represents the best-fit based on the log (*time to failure*) versus log (*applied interlaminar shear stress*) relation, which will be discussed later. A relatively large scatter in time to failure is noted, similar to the feature shown in many CMCs and advanced monolithic ceramics subjected to stress rupture in tension or flexure at elevated temperatures. Statistical aspects of the data in stress rupture will be described in the Discussion section in conjunction with those in constant stress rate.

(a)   (b)
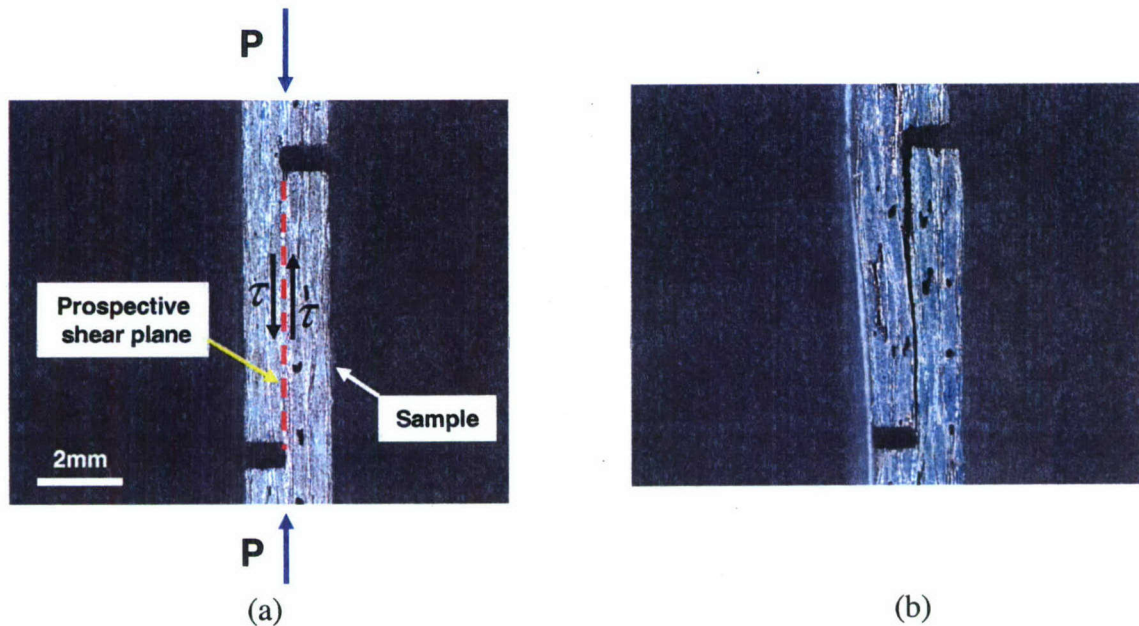
Figure 3: Examples of (a) an as-machined DNS test specimen and (b) a specimen tested in interlaminar shear stress rupture at 17.8 MP at 1316°C in air. The material was Hi-Nic SiC/SiC composite.
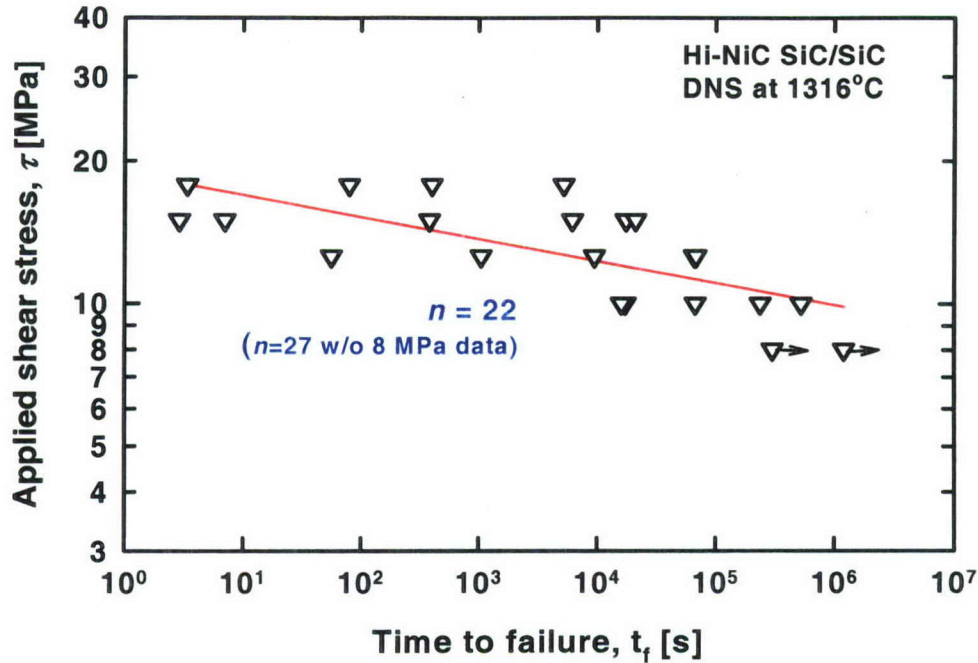
Figure 4: Results of stress rupture testing for Hi-Nic SiC/SiC composite in Interlaminar shear at 1316°C in air. The solid line represents the best fit.

Some extents of creep deformation were observed in specimens particularly those tested at the lowest applied stress of 8 MPa, as shown from the displacement-time curves in figure 5. A total of approximate 100 μm (for Specimen 'A') to 300 μm (for Specimen 'B') of creep deformation in compression was observed for the whole period of test times. Most of the deformation was associated with compression in notch sections. The runout specimen (Specimen 'A') that did not fail up to 380 hr showed lateral but opposite buckling-associated creep deformation of the upper and lower parts of the specimen, as shown in figure 6. Each lower or upper part of the specimen was subjected to some progressive lateral deformation due to its buckling hinged at the notched region and at load point. This was evidently a limitation encountered in the long-term DNS stress rupture tests at lower stress levels (≤ 8 MPa). More rigorous provisions such as use of better creep-resistant antibuckling guides together with well-finished test-specimen surfaces could mitigate this undesirable lateral flexure-associated creep deformation. However, it should be mentioned that some changes in stress states at the notch regions could be inevitable when significant creep takes place around the stress concentrated notches.
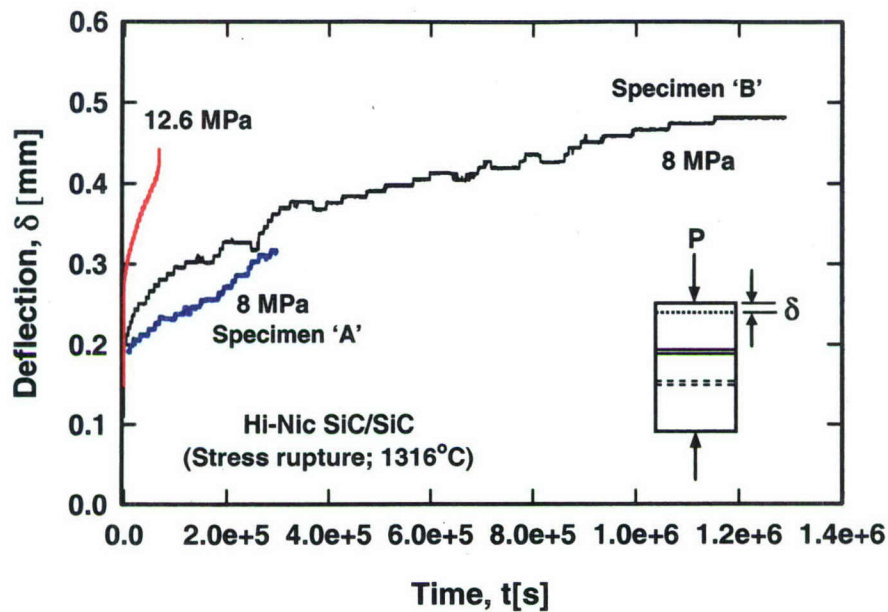
Figure 5: Creep deflection of DNS specimens subjected to stress rupture at an interlaminar shear stress of 8 and 12.6 MPa at 1316°C in air for Hi-Nic SiC/SiC composite.
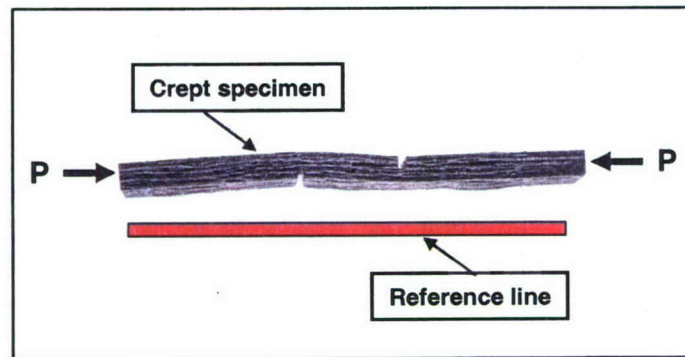

Figure 6: Example of lateral creep deformation due to buckling for a specimen subjected to stress rupture in interlaminar shear at 1316°C in air for Hi-Nic SiC/SiC composite. Applied shear stress=8 MPa; test time=380 hr.

Fracture surfaces of specimens tested showed discoloration due to oxidation, which appeared to be greater for lower stress-tested specimens than for higher stress-tested specimens. Specimens tested at lower stresses showed typically smooth and clean fracture surfaces with little broken fibers and debris; whereas, specimens tested at higher stresses revealed increased damage with fiber breakage, as shown in figures 7 and 8. This implies that interface-associated failure through SCG or damage accumulation would be more dominant at the lower stress regime than at the higher stress regime. Time for SCG along the interfaces between fiber tows and matrices was

not sufficient at higher stresses, resulting in a phenomenon of 'fast fracture' by accompanying rough fracture surfaces with increased fiber and matrix damage.
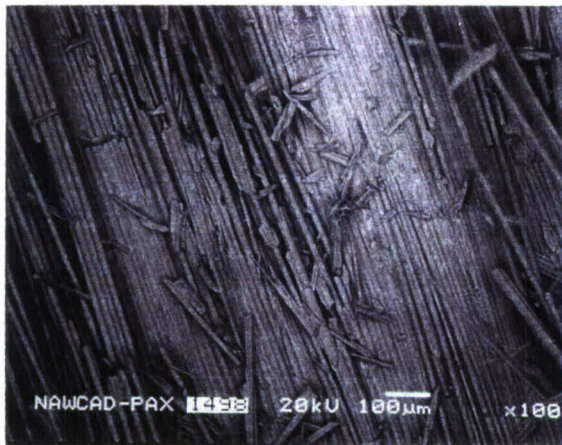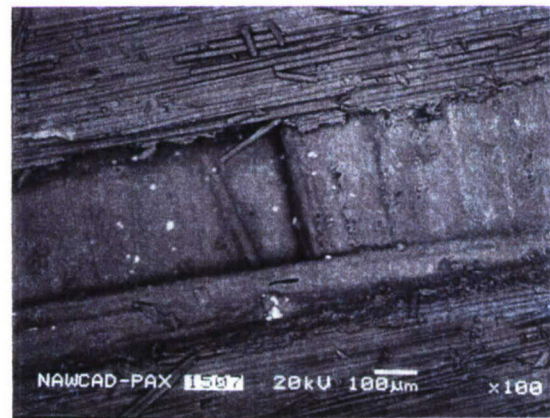

(a)

(b)

Figure 7: Fracture surface of a specimen subjected to stress rupture in interlaminar shear tested at a high stress of 17.8 MPa at 1316°C in air for Hi-Nic SiC/SiC composite (time to failure = 3 sec). (a) Overall and (b) a matrix-rich region showing imprints of fibers.

(a)

(b)

Figure 8: Fracture surface of a specimen subjected to stress rupture in interlaminar shear tested at a low stress of 10 MPa at 1316°C in air for Hi-Nic SiC/SiC composite (time to failure = 524000 sec (146 hr)). (a) Overall and (b) a 'blind' region showing insufficient matrix filling.

Figure 7(b) also exhibits well-preserved imprints of fibers on the mating matrix, showing an important aspect of interlaminar shear failure involved with CMCs. The small round or elliptical holes lined up with the perpendicular fibers beneath, as seen in figure 7(b), are an indication of

direct fiber-to-fiber contacts, attributed to insufficient infiltration of matrix material between the two adjacent plies. It was also observed from fracture surfaces that there were some 'blind' regions where no matrix or silicon was filled between plies or tows, resulting in significant gaps or voids or pores in the composite, as shown in figure 8(b). This certainly contributes to decreased interlaminar shear or tensile properties.

Figure 9 depicts the cross-sectional views along the fractured (sheared) surfaces for high (17.8 MPa) and low (10 MPa) stress-tested specimens. Fiber tows, matrix, and big voids are also seen from the figure. The specimen tested at a high stress of 17 MPa, figure 9(a), exhibited one crack within a tow. By contrast, for the specimen tested at a low stress of 10 MPa, figure 9(b), there were multiple, at least four, cracks close to tow-to-tow interfaces. This might indicate again that SCG or damage accumulation/propagation at interfaces would have been more predominant at lower stresses than higher stresses, as also observed from the fracture surfaces in figures 9 and 10. However, it should be noted that multiple cracks are not necessarily a result of lower stresses. Multiple cracks are frequently observed as a pattern of crack branching for many brittle solids such as monolithic ceramics and glasses subjected to significantly high energy or high applied stresses [14].
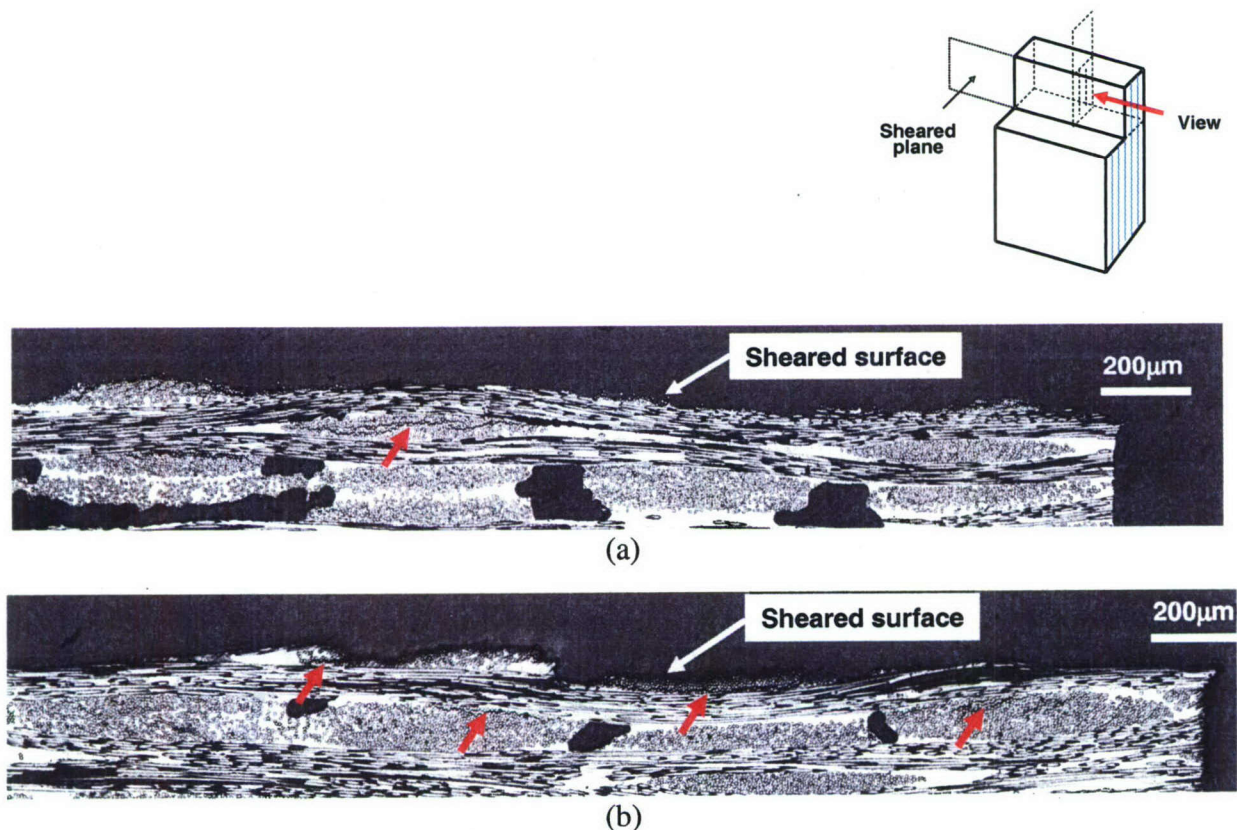

Figure 9: Cross-sectional views of sheared planes of specimens subjected to stress rupture in interlaminar shear at 1316°C in air for Hi-Nic SiC/SiC composite. (a) Applied stress = 17.8 MPa and (b) 10 MPa. Arrows indicate cracks.
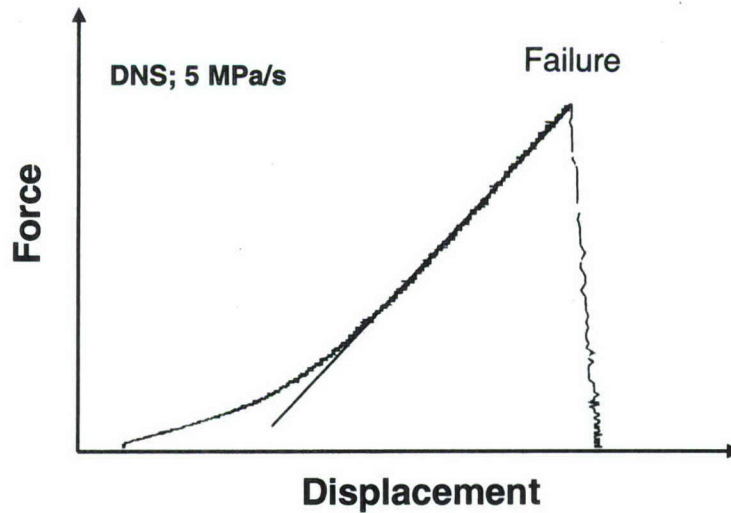
Figure 10: Typical force-displacement curve of a DNS specimen tested at a stress rate of 5 MPa/s in interlaminar shear at 1316°C in air for Hi-Nic SiC/SiC composite.

3.2 CONSTANT STRESS-RATE TEST

Without exception, all specimens tested in constant stress-rate loading failed in interlaminar shear, similar in mode to the one already shown in figure 3. Most specimens exhibited a linear relationship between force and displacement, although the specimen tested at the lowest test rate of 0.0005 MPa/s exhibited some nonlinearity in its force-displacement curve because of some creep deformation. In general, the linearity in force-displacement curves has been typified of many CMCs in interlaminate shear testing at either ambient or elevated temperatures [5,6,7], which is in contrast to in-plane tensile testing where matrix cracking and subsequent damage accumulation are exemplified in the curves. A typical example of force-displacement behavior of a specimen tested at 5 MPa/s is illustrated in figure 10.

The results of constant stress-rate testing are presented in figure 11, where interlaminar shear strength was plotted as a function of applied shear stress rate in a log-log scheme. The solid line represents the best fit. Despite some scatter in the data, the overall interlaminar shear strength decreased with decreasing applied shear stress rates. This phenomenon of strength degradation with decreasing test rate, often called SCG or dynamic fatigue when referred to monolithic brittle materials in tension or in flexure [12,13], is an evidence of SCG or damage accumulation occurring at the fiber-matrix interfaces along a respective shear plane under loading. This type of life limiting behavior, associated with strength degradation in interlaminar shear, was also observed for other CMCs including SiC/SiCs, SiC/MAS, C/SiC, and SiC/BSAS at elevated temperatures [6,7]. Based on the results of figures 4 and 11, it can be stated that life limiting behavior of the composite occurred in interlaminar shear, either in constant loading (stress rupture) or in time varying loading (constant stress rate).
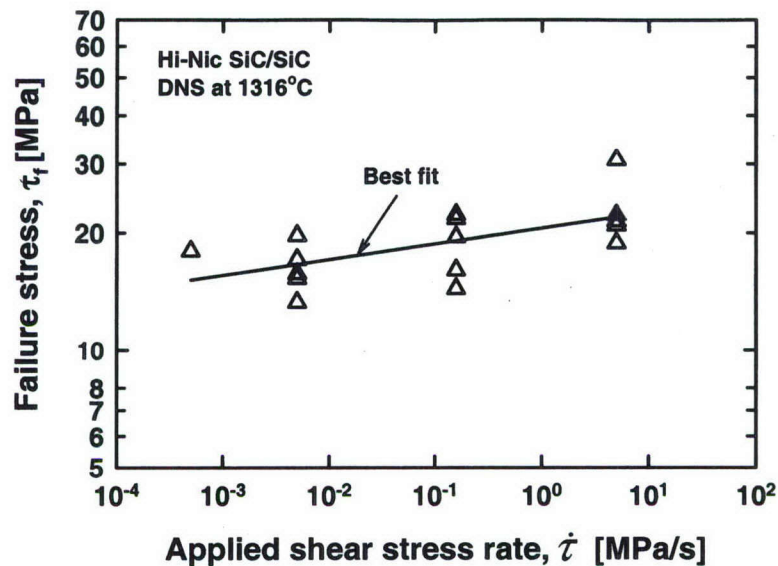
Figure 11: Results of failure stress (interlaminar shear strength) as a function of applied shear stress rate determined in constant stress-rate testing at 1316°C in air for Hi-Nic SiC/SiC composite. The solid line represents the best fit.

Unlike those tested in stress rupture, the specimens tested in constant stress rates did not show any significant difference in discoloration of fracture surfaces between high and low stress-rate tested specimens. This was due to a relatively short test time (≤ 1 hr) in constant stress-rate testing. Figure 12 represents fracture surface of a specimen tested at a high test rate of 5 MPa/s, which shows somewhat rougher surfaces, when compared with that of low rate-tested specimens, with tow breakage, broken fibers, and matrix/fiber debris. Figure 12(a) also shows both 'blind' ('A') and well-contacted ('B') regions between fiber tows and matrix. The well-contacted region is typified of many imprints of fibers on matrix, while the 'blind' region is characterized with little fiber imprints therein. Detailed examinations of broken fibers indicated that individual fibers failed in tension or in flexure leaving shear lips, as can be seen in figure 12(b).
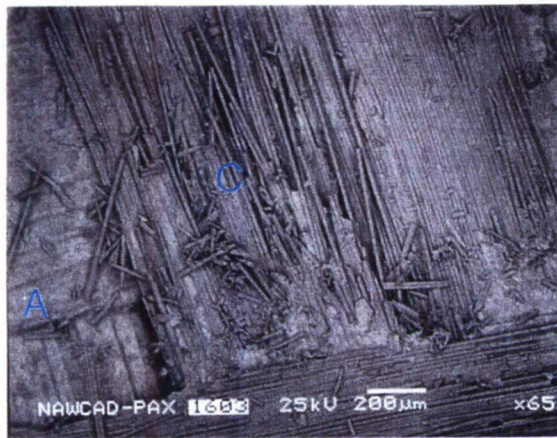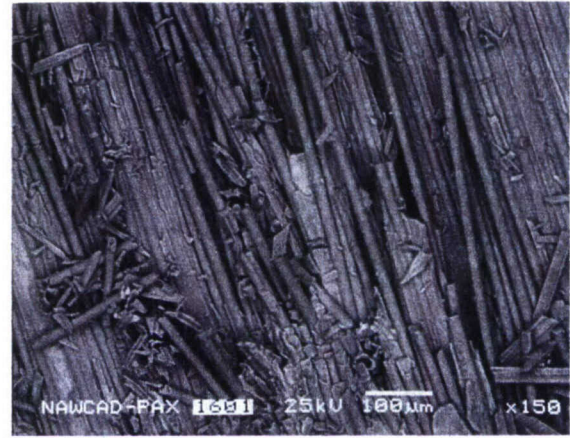
(a)

(b)

Figure 12: Fracture surface of a specimen subjected to constant stress rate testing in interlaminar shear at a high stress rate of 5 MPa/s at 1316°C in air for Hi-Nic SiC/SiC composite (shear strength= 22 MPa). (a) Overall and (b) enlarged region of 'C'.

Figure 13 represents fracture surface of a specimen tested at a low test rate of 0.005 MPa/s. The fracture surface was somewhat smoother with less damage in fibers and matrix than those of specimens tested at higher test rates, as also seen from the specimens subjected to stress rupture. A 'blind' region (designated 'A') is also seen in figure 13. A rare case of fiber failure in a plucked-up mode (z-direction) is shown in figure 14, where both regions of fiber pullouts (lower region) and brittle failure (upper region) are identified. The rough surface associated with fiber-tow breakage in the z-direction would give significant friction, resulting in increased crack growth resistance when a Mode II crack is to propagate. CMCs with rough interlaminar crack planes exhibited increased crack growth resistance in Mode II with rising R-curve [10].

(a) (b)

Figure 13: Fracture surface of a specimen subjected to constant stress rate testing in interlaminar shear at a low stress rate of 0.005 MPa/s at 1316°C in air for Hi-Nic SiC/SiC composite (shear strength= 13 MPa). (a) Overall and (b) enlarged region of 'C'.
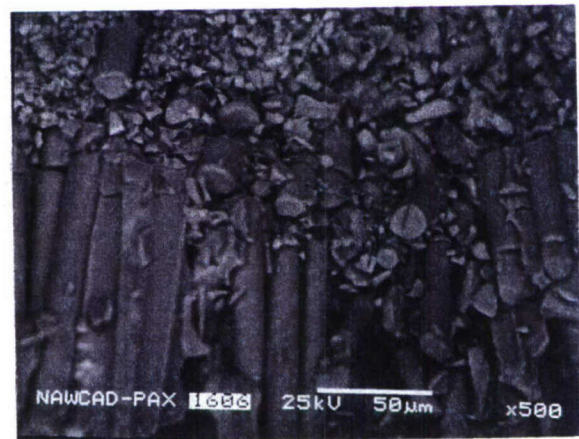
(a) (b)

Figure 14: Fracture surface showing fibers (tow) breakage in a z-direction for a specimen subjected to constant stress-rate testing in interlaminar shear at 0.005 MPa/s at 1316°C in air for Hi-Nic SiC/SiC composite (shear strength=13 MPa). (a) Overall and (b) enlarged.

Fracture surfaces of specimens tested in constant stress-rate loading, in general, exhibited more damage in fibers, tows, and matrix than those tested in stress rupture loading. This may be due to the fact that the extension of SCG or damage accumulation was insignificant in constant stress-rate loading because of shortened test time, as compared to long-term testing in stress rupture. The enhanced degree of SCG would yield smoother fracture surfaces, and vice versa, as also observed in many brittle materials such as glasses and monolithic ceramics. However, it should be noted that unlike homogeneous brittle solids, CMCs usually give a challenge in fractography to characterize the origin, nature, and type of strength controlling flaws and the extension of SCG.

4. DISCUSSION

4.1 ASSESSMENT OF LIFE LIMITING PROPERTY IN STRESS RUPTURE

A phenomenological SCG model proposed previously [6,7] will be applied to the stress rupture data determined in this study for the Hi-Nic SiC/SiC composite and will be validated with the constant stress-rate test data.[1] The proposed SCG model in Mode II was similar in expression to the power-law relation in Mode I loading [15], and takes a following, empirical formulation [6,7]:

$$v_s = \frac{da}{dt} = \alpha_s \, (K_{II} / K_{IIc})^{n_s} \tag{3}$$

where v_s, a, t, K_{II}, and K_{IIc} are crack-growth rate in interlaminar shear, crack size, time, Mode II stress intensity factor, and Mode II fracture toughness, respectively. α_s and n_s are life limiting (or SCG) parameters in interlaminar shear. The above formulation was fracture-mechanics based, in which an explicit, dominant crack residing at interlaminar fiber-matrix interfacial regions is assumed to start and grow subcritically, eventually leading to an instability condition. It may be arguable as to whether a term 'crack' or fracture mechanics concept can be used for CMCs since fracture origin and subsequent crack growth region are not typically observable from fracture surfaces, due to their architectural nature. So, in principle, any other approach such as creep or damage associated mechanics, if appropriate, can be used as an alternative to life modeling.

The generalized expression of K_{II} along the crack front of a penny or half-penny shaped crack subjected to shear loading either on crack planes or on remote material body can take the following form [16]:

$$K_{II} = Y_s \tau \, a^{1/2} f(\theta, \varphi) \tag{4}$$

where Y_s is a crack geometry factor related to a function of $f(\theta, \varphi)$ with the angles θ and φ being related to load and a particular point of the crack front, as shown in figure 15. τ is the applied interlaminar shear stress. Using Equations (3) and (4) together with some mathematical manipulations, one can obtain time to failure (t_f) as a function of applied shear stress, as done for brittle materials in Mode I loading [17,18]:

$$t_f = D_s [\tau]^{-n_s} \tag{5}$$

---

[1] Typically, a conventional practice of life prediction of brittle materials is undertaken such that life prediction parameters are first estimated from the data determined in constant stress rate testing, a life prediction is then made with appropriate relations, and then the prediction is compared with stress rupture data. However, in this work, the practice was reversed intentionally by beginning with stress rupture data to evaluate life prediction parameters, making a strength-degradation prediction, and then by comparing the prediction with constant stress-rate data. Any of the methods, in principle, should yield the similar results.

where

$$D_s = B_s \, [\tau_i]^{n_s - 2} \tag{6}$$

where $B_s = 2K_{IIc}[\alpha_s Y_s^2 (n_s - 2)]$, τ_i is the inert shear strength that is defined as a strength with no SCG, and the geometry function is simplified as $f(\theta, \varphi) = 1$ in the case of DNS loading for an infinite material body.[2] Equation (5) can be expressed in a more convenient form by taking logarithms of both sides

$$\log t_f = -n_s \log \tau + \log D_s \tag{7}$$

which is identical in form to the case in Mode I loading used in monolithic ceramics [17,18]. Life limiting parameters n_s and D_s in interlaminar shear can be determined based on Equation (7), respectively, from the slope and the intercept of a linear regression analysis of the log (*individual applied interlaminar shear stress with units of MPa*) versus log (*individual time to failure with unit of second*) data, figure 4. The parameter α_s is then evaluated using the above B_s relation with appropriate parameters/constants. Using the data in figure 4 and the linear regression, the life limiting parameters of the composite were found to be

$$n_s = 21.5 \text{ and } \log D_s = 27.5 \tag{8}$$

with the coefficient of correlation of curve fit of $r_{coef} = 0.7303$. The best fit was indicated as a solid line in the figure. As seen from figure 4, statistically good agreement exists between the model and the data, although the data scatter in time to failure was in a few orders of magnitude, which is typical of most brittle materials in stress rupture or in cyclic fatigue.

---

[2] The geometry factor $Y_s f(\theta, \varphi)$ can change as a crack grows through a SCG process if the crack becomes finite relative to the material body (test coupon). This change, however, occurs typically close to an instability for a material exhibiting a life limiting parameter $n \geq 20$, resulting in little change in the value of time to failure (or strength in constant stress-rate loading) [19]. Hence, the approach using $f(\theta, \varphi) = 1$ with a constant Y_s in this work is reasonable throughout the lives of test coupons.
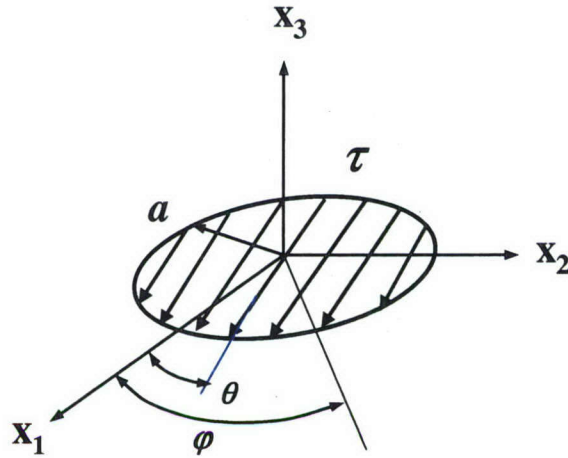
Figure 15: An assumed penny-shaped crack arbitrarily located at matrix-fiber interfaces
in CMCs, subjected to equal and opposite interlaminar shear stresses τ acting
on both surfaces of a crack.

The empirical SCG formulation of brittle homogeneous solids subjected to Mode I is
expressed as [15]:

$$v = \frac{da}{dt} = \alpha \, (K_I \, / \, K_{Ic})^n \qquad\qquad (9)$$

where K_I and K_{Ic} are stress intensity factor and fracture toughness, respectively, both in Mode I
loading, and α and n are SCG parameters in Mode I. It has been generally categorized for brittle
materials under Mode I that life limiting susceptibility is significant for $n<30$, intermediate for
$30<n<70$, and insignificant for $n>70$. Hence, in terms of this categorization, the Hi-Nic SiC/SiC
composite with $n_s=22$ can be said to exhibit *significant* life limiting in interlaminar shear at
$1316°C$ in air.

4.2 VERIFICATION

The proposed crack growth formulation, Equation (3), indicates that for a given
material/environmental condition, crack velocity depends on K_{II} so that in principle the life
limiting parameters can be determined in any loading configuration which is either static, cyclic,
or any time varying. Therefore, it should be possible to make a life prediction from one loading
configuration to another provided that the same failure mechanism is operative. In this section,
the life limiting parameters that were determined in stress rupture will be used to predict the
strength degradation behavior in constant stress-rate loading and to validate the proposed crack
growth model. Note that strength degradation with respect to decreasing test rate is another form
of life limiting phenomena, in which the degree of crack growth is a reflection of strength
degradation. Using Equations (5) and (6) with some mathematical manipulations, a relationship

17

between interlaminar shear strength (τ_f) and applied shear stress rate ($\dot{\tau}$) can be derived as follows:

$$\tau_f = D_d \, [\dot{\tau}]^{\frac{1}{n_s+1}} \tag{10}$$

where

$$D_d = [D_s \, (n_s + 1)]^{\frac{1}{n_s+1}} \tag{11}$$

Equation (10) shows that interlaminar shear strength is a function of applied shear stress rate for a given material/temperature/environment. Therefore, a strength prediction requires only the life prediction parameters n_s and D_s that are to be estimated from stress rupture data.

The resulting prediction of interlaminar shear strength, based on Equation (9) with the estimated parameters n_s and D_s, is presented as a solid line in figure 16. Despite some scatters in shear strength, the prediction was in good agreement with the best fit of the experimental data. The discrepancy in shear strength between the prediction and the data were only 6% to 9%. Particularly, the life limiting parameter of $n_s=22$ estimated from stress rupture was in excellent agreement with $n_s=24$ that was evaluated from the constant stress-rate data by a regression analysis of $\log(\tau_f)$ versus $\log(\dot{\tau})$. The parameter D_d was also in good agreement with log D_d =27.5 and 31.4, estimated from the stress rupture and the constant stress-rate data, respectively. These results indicated that the *overall* governing failure mechanism of the composite subjected to interlaminar shear remained almost unchanged, regardless of loading configurations, and that the failure mechanism could be described by the power-law type of crack growth formulation, Equation (3). Statistically, the prediction made above represents a failure probability of approximately 50%. Of course, different levels of failure probability in shear strength, which accounts for the strength scatter, can be made if Weibull strength distribution of τ_i is known, as implied from the parameter D_s (Equation (6)).
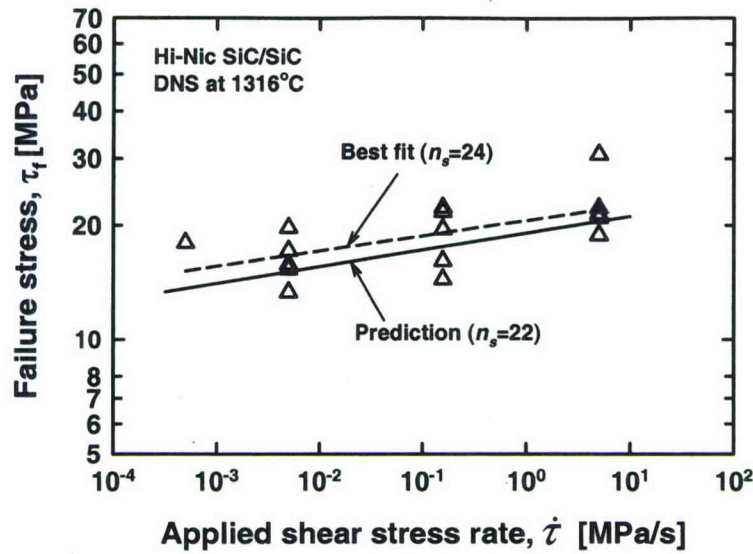
Figure 16: Comparison in interlaminar shear strength between the predicted and the actual data for Hi-Nic SiC/SiC composite in interlaminar shear tested at 1316°C in air.

4.3 STATISTICAL ASPECTS OF DATA

As stated in the preceding section, good agreement in strength/life predictions in interlaminar shear was found between the two different loading conditions, indicative of an almost same failure mechanism prevailing in the composite regardless of loading configurations. This also shows that the Hi-Nic SiC/SiC composite in interlaminar shear behaves very similar in life limiting to homogeneous brittle materials such as glasses and advanced ceramics in Mode I. This prompts to check if statistical behavior of the composite's experimental data follows a pattern similar to that of brittle materials. It has been shown that under Mode I loading, brittle materials, when exhibit one dominant failure mechanism independent of the type of loading, yield a relationship in Weibull modulus between strength and time-to-failure, as follows [18][3];

$$m_s \approx \frac{m_d}{n-2} \tag{12}$$

where m_s and m_d are Weibull modulus in time-to-failure distributions (in stress rupture) and Weibull modulus in strength distributions (in constants stress rate), respectively, and n is the major life limiting parameter in Equation (10). It is evident from Equation (12) that the greater parameter n yields the greater data scatter in time to failure, and vice versa. Also, the scatter is always greater in time to failure than in strength for most of brittle materials that typically exhibit $n \geq 20$.

---

[3] The relationship can be derived from Equations (5) and (10) if Weibull distribution of inert shear strength (τ_i) is given.

Weibull modulus in interlaminar shear strength of the composite ranged from $m_d = 5.5$ to 8.0 over the three stress rates used, resulting in an average of $m_d = 6.5 \pm 1.3$. Use of Equation (11) with $m_d = 6.5$ and $n \equiv n_s = 22$ yielded a predicted value of $m_s = 0.33$. Weibull modulus in time-to-failure estimated at the four different levels of applied shear stresses was in a range of $m_s = 0.3$ to 0.7 with an average of $m_s = 0.44 \pm 0.18$. As a consequence, the relation in Equation (12) is in reasonable agreement with the data, applicable even to the CMC in interlaminar shear. Figure 17 shows two-parameter Weibull plots in interlaminar shear strength and time to failure, and compares the time-to-failure data with the predicted curves with $m_s = 0.33$. Except for $\tau = 10$ MPa, this result, despite the limited number of specimens used (typically five), is surprising since the composite, which is so complex in microstructure and architecture, behaves as if it were a homogeneous, isotropic material under Mode I loading. These statistical aspects of the composite draw again a conclusion that the governing failure mechanism might have remained unchanged either in stress rupture or in constant stress rate. Note that the relation in Equation (12) was derived with a basic assumption that a failure mechanism (Equation (9)) remains consistent regardless of loading configurations [18]. Certainly, use of more test specimens could verify better the validity of the relation of Equation (12) for the composite.
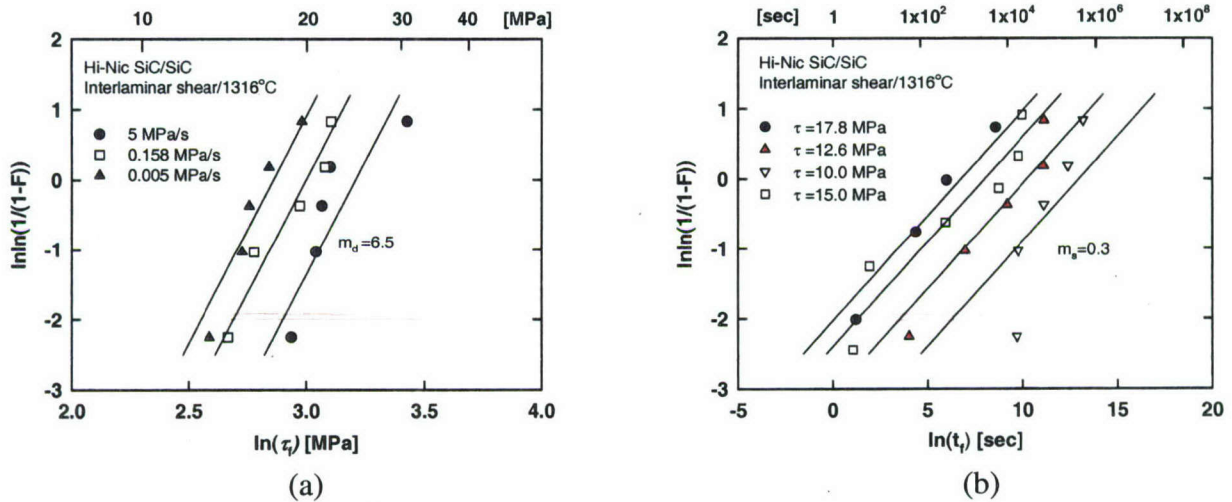
Figure 17: Weibull distributions of interlaminar shear strength and time-to-failure for Hi-Nic SiC/SiC composite in interlaminar shear tested at 1316°C in air. (a) Weibull interlaminar shear-strength distributions in constant stress-rate testing. The solid lines represent the fits with an average m_d=6.5. (b) Weibull time-to-failure distributions in stress rupture. The solid lines represent the predictions based on m_s=0.3, determined from Equation (12) with m_d=6.5.

4.4 LIFE LIMITING BEHAVIOR IN INTERLAMINAR SHEAR FOR OTHER CMCs

Several other CMCs have been used previously to assess their life limiting properties in interlaminar shear at elevated temperatures mainly under constant stress-rate loading [6,7]. The results are again summarized in figure 18. Table 1 summarizes the major life prediction parameter n_s obtained from these composites. Glass matrix composites such as SiC/MAS and SiC/BSAS exhibited a high susceptibility to life limiting with $n_s = 8$-11, primarily due to the enhanced viscous flow at elevated temperatures by glassy phases in matrix. The C/SiC composite showed significant life limiting behavior with $n_s = 2$, attributed to the oxidation of carbon fibers in an air environment. The MI Sylramic™ SiC/SiC composite presented a high resistance to life limiting at the higher shear stress-rate regime ($\geq 5 \times 10^{-3}$ MPa/s) with $n_s = 90$ but exhibited a significantly increased susceptibility at the lower shear stress-rate regime ($< 5 \times 10^{-3}$ MPa/s) with $n_s = 3$. The SiC/SiC ('90 vintage) composite exhibited a good life-limiting resistance with $n_s = 90$ as well and greater strength than the Sylramic SiC/SiC composite. However, a question arises as to whether the SiC/SiC composite, like the Sylramic SiC/SiC, would exhibit a similar strength degradation if further decreasing stress rates ($< 0.5 \times 10^{-3}$ MPa/s) are used.
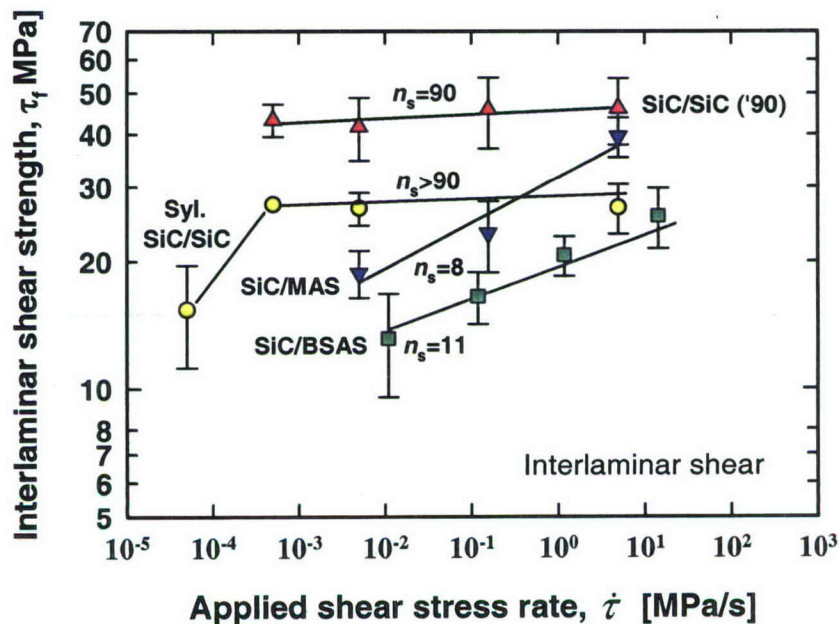

Figure 18: Summary of constant stress-rate testing for various CMCs in interlaminar shear at elevated temperatures in air [5,6]. Test specimens were all in DNS configurations.

Table 1: Life prediction parameter n_s for various continuous fiber-reinforced CMCs determined in constant stress-rate testing in interlaminar shear at elevated temperatures in air. The parameter n in in-plane tension is included for comparison.

CMCs	Test Temperature ($^{\circ}$C)	n_s (Interlaminar shear)[1] [6,7]	n (In-plane tension)[2] [20,21]
SiC/MAS (2D)	1100	8	18
SiC/BSAS (1D)	1100	11	7
C/SiC (2D woven)	1200	2	6
SiC/SiC (2D woven; '90)	1200	90	20
Sylramic SiC/SiC (2D woven)	1316	90/3*	-
Hi-Nic SiC/SiC (2D woven) [this study]	1316	24	-

NOTES: (1) Typical shear area in DNS test specimens was W x L_n = 13 mm x 6 mm, except for SiC/BSAS which was 4 mm x 5 mm.

   (2) All dogboned test specimens were used in in-plane tensile testing with a gage section 2-3 mm thick, 10 mm wide, and about 20-30 mm long.

   * For Sylramic™ SiC/SiC composite, the value of n_s=90 is for higher stress-rate regime ($\geq 5 \times 10^{-3}$ MPa/s) and n_s=3 for lower stress-rate regime ($<5 \times 10^{-3}$ MPa/s) [7].

Table 1 also includes the Mode I life prediction parameter n for some of the CMCs determined in in-plane tension by constant stress-rate testing at elevated temperatures [20,21]. It may not be reasonable to compare directly between n_s and n since major failure mechanism(s) differs: Interlaminar shear strength is likely to be controlled by fiber-matrix interfaces, whereas in-plane tensile strength is governed mainly by fibers. A seemingly general trend, except for the SiC/SiC composite, is that lower n results in lower n_s. However, care must be exercise to draw any conclusions regarding the n versus n_s relation.

4.5 LIFE PREDICTION METHODOLOGY OF CMCs IN INTERLAMINAR SHEAR

The results of this work indicate that the governing failure mechanism in interlaminar shear would not differ significantly either in stress rupture or in constant stress-rate loading and that the *overall* failure mechanism could be described by the power-law type of crack growth formulation, Equation (3). The results also indicate that stress rupture or constant stress-rate testing can be utilized as a life-prediction test methodology to determine quantitatively the phenomenological life prediction parameters of CMCs even in interlaminar shear. Stress rupture testing gives more realistic life data but it gives increased data scatter so that more test specimens are required, which is time consuming particularly at lower applied stresses. By contrast, constant stress-rate testing gives merits in simplicity, test economy (short test times), and less data scatter over other stress rupture or cyclic fatigue testing thus allowing less number of test specimens which can be seen from Equation (12). Therefore, as far as one prevailing mechanism is associated with failure, constant stress-rate testing is a more preferable choice over stress rupture testing. However, caution should be exercised when more than one failure mechanism combined with SCG, creep, and environmental degradation, etc., occurs simultaneously. In this case, use of constant stress-rate testing should be limited for the case of a short period of lives.

An accelerated test technique has been developed to save test time in constant stress-rate, life prediction testing primarily for monolithic ceramics and glasses in tension or flexure at both ambient and elevated temperatures [12,13,22]. The technique has been applied to CMCs in in-plane tension at elevated temperatures and verified its effectiveness to CMCs [20,21]. Although not certain, the accelerated technique might be applicable to constant stress-rate testing in interlaminar shear thus to save a significant amount of test times.

Although exploration of detailed failure mechanism(s) is beyond the scope of this work, a more detailed microscopic failure analysis regarding matrix/fiber interaction, matrix cracking, localized SCG, creep, and environmental effects [23-25], is still needed. It should be kept in mind that the phenomenological model proposed here may incorporate other operative models such as viscous sliding, void nucleation, and coalescence, etc., which can be all covered under a generic term of delayed failure, SCG, fatigue, creep, or damage initiation/accumulation [26].

Finally, the results of this work also suggest that care must be exercised when characterizing elevated-temperature, interlaminar shear strength of composite materials. This is due to the fact that if a material exhibits a life limiting phenomenon, elevated-temperature interlaminar shear strength has a relative meaning because interlaminar shear strength depends on which test rate one chooses. Therefore, at least two or three test rates including high and low are recommended to better characterize interlaminar shear strength behavior of a composite material, as suggested previously for the determination of ultimate tensile strength of CMCs and monolithic advanced ceramics at elevated temperatures [20,21,27]. Another important note to point out is that since life limiting of CMCs occurs not only in tension but in interlaminar shear, modification or development of any integrated reliability/life prediction code should take into account a phenomenon of time-dependent interlaminar shear failure at elevated temperatures.

THIS PAGE INTENTIONALLY LEFT BLANK

5. CONCLUSIONS

Life limiting behavior of Hi-Nic SiC/SiC composite was assessed in interlaminar shear at 1316°C in air. The following conclusions were made:

1) The composite exhibited a significant life limiting susceptibility with n_s=22-24, estimated based on a proposed phenomenological crack growth model.

2) The proposed model exhibited good agreement between the prediction and the experimental data, and between the shear strength data and the strength prediction from the stress rupture data.

3) Weibull modulus of the composite was found to be around 6 and 0.3 in shear strength and time to failure, respectively. A statistical aspect in Weibull modulus, observed for many isotropic brittle materials, existed between shear strength and time-to-failure data.

4) The governing failure mechanism(s) remained almost unchanged either in stress rupture or in constant stress rate loading. This indicates that constant stress-rate testing could be a possible means of life prediction test methodology in interlaminar shear when short lifetimes of components are anticipated.

5) Due to the life limiting behavior occurring at elevated temperatures, shear strength of composites depends on test rate, so that two or more test rates are required to completely characterize elevated-temperature shear strength behavior of a composite.

6. FUTURE WORK

The current experimental work was conducted at an elevated temperature only in air. It is necessary to use appropriate aeroengine environments to better describe life limiting behavior of the material in interlaminar shear. This may require burner rig, salt fog, and/or sand infiltration testing, which will be the subject of future work. A further experimental study is sought to validate if an accelerated test technique could be applicable to CMCs in interlaminar shear at elevated temperatures. Furthermore, additional tests over a wide range of temperatures would be necessary to identify in more detail the failure mechanisms because an activation energy could then be established and a temperature-compensated time method could be used to help fit experimental data with an increased accuracy.

THIS PAGE INTENTIONALLY LEFT BLANK

REFERENCES

1. P. Brondsted, F. E. Heredia, and A. G. Evans, "In-Plane Shear Properties of 2-D Ceramic Composites," *J. Am. Ceram. Soc.*, **77**[10] 2569-2574 (1994).

2. E. Lara-Curzio and M. K. Ferber, "Shear Strength of Continuous Fiber Ceramic Composites," ASTM STP 1309, p. 31, American Society for Testing and Material, West Conshohocken, PA (1997).

3. N. J. J. Fang and T. W. Chou, "Characterization of Interlaminar Shear Strength of Ceramic Matrix Composites," *J. Am. Ceram. Soc.*, **76**[10] 2539-2548 (1993).

4. Ö. Ünal and N. P. Bansal, "In-Plane and Interlaminar Shear Strength of a Unidirectional Hi-Nicalon Fiber-Reinforced Celsian Matrix Composite," *Ceramics International*, **28** 527-540 (2002).

5. S. R. Choi and N. P. Bansal, "Interlaminar Tension/Shear Properties and Stress Rupture in Shear of Various Continuous Fiber-Reinforced Ceramic Matrix Composites," *Advances in Ceramic Matrix Composites XI*, Edited by N. P. Bansal, J. P. Singh, and W. M. Kriven, The American Ceramic Society, Westerville, Ohio; *Ceramic Transactions*, **175** 119-134 (2006).

6. S. R. Choi and N. P. Bansal, "Shear Strength as a Function of Test Rate for SiC_f/BSAS Ceramic Matrix Composite at Elevated Temperature," *J. Am. Ceram. Soc.*, **87**[10] 1912-1918 (2004).

7. S. R. Choi, N. P. Bansal, A. M. Calomino, and M. J. Verrilli, "Shear Strength Behavior of Ceramic Matrix Composites at Elevated Temperatures," *Advances in Ceramic Matrix Composites X*, Edited by J. P. Singh, N. P. Bansal, and W. M. Kriven, The American Ceramic Society, Westerville, Ohio; *Ceramic Transactions*, **165** 131-145 (2005).

8. D. Brewer, "HSR/EPM Combustor Materials Development Program," *Mat. Sci. Eng.*, **A261** 284-291 (1999).

9. ASTM C 1259, "Test Method for Dynamic Young's Modulus, Shear Modulus, and Poisson's for Advanced Ceramics by Impulse Excitation of Vibration," *Annual Book of ASTM Standards*, Vol. 15.01, American Society for Testing and Materials, West Conshohocken, PA (2006).

10. S. R. Choi and R. W. Kowalik, "Interlaminar Crack Growth Resistances of Various Ceramic Matrix Composites in Mode I and Mode II Loading," ASME Turbo Expo 2007, 14-17 May 2007, Montreal, Canada; *ASME Paper No.* GT2007-27080.

11. ASTM C 1425, "Test Method for Interlaminar Shear Strength of 1-D and 2-D Continuous Fiber-Reinforced Advanced Ceramics at Elevated Temperatures," *Annual Book of ASTM Standards*, Vol.15.01, American Society for Testing and Materials, West Conshohocken, PA (2006).

12. ASTM C 1368, "Standard Test Method for Determination of Slow Crack Growth Parameters of Advanced Ceramics by Constant Stress-Rate Flexural Testing at Ambient Temperature," *Annual Book of ASTM Standards*, Vol. 15.01, American Society for Testing and Materials, West Conshohocken, PA (2006).

13. ASTM C 1465, "Standard Test Method for Determination of Slow Crack Growth Parameters of Advanced Ceramics by Constant Stress-Rate Flexural Testing at Elevated Temperatures," *Annual Book of ASTM Standards*, Vol. 15.01, American Society for Testing and Materials, West Conshohocken, PA (2006).

14. S. R. Choi and J. P. Gyekenyesi, "Crack Branching and Fracture Mirror Data for Glasses and Advanced Ceramics," NASA TM 206536, National Aeronautics and Space Administration, Glenn Research Center, Cleveland, OH (1998).

15. A. G. Evans, "Slow Crack Growth in Brittle Materials under Dynamic Loading Condition," *Int. J. Fracture*, **10** 251-259 (1974).

16. H. Tada, P.C. Paris, and G. R. Irwin, The Stress Analysis of Cracks Handbook, p. 418, ASME, NY (2000).

17. ASTM C 1576 "Standard Test Method for Determination of Slow Crack Growth Parameters of Advanced Ceramics by Constant Stress Flexural Testing (Stress Rupture) at Ambient Temperature," *Annual Book of ASTM Standards*, Vol. 15.01, American Society for Testing and Materials, West Conshohocken, PA (2006).

18. J. E. Ritter, N. Bandyopadhyay, and K. Jakus, "Statistical Reproducibility of the Dynamic and Static Fatigue Experiments," *Ceramic Bulletin*, **60**[8] 798-806 (1981).

19. (a) S. R. Choi and G. P. Gyekenyesi, "Specimen Geometry Effect on the Determination of Slow Crack Growth Parameters of Advanced Ceramics in Constant Flexural Stress-Rate Testing at Elevated Temperatures," *Ceram. Eng. Sci. Proc.*, **20**[3], 525-534 (1999). (b) S. R. Choi and J. P. Gyekenyesi, "Slow Crack Growth Analysis of Brittle Materials with Finite Thickness Subjected to Constant Stress-Rate Testing," *J. Mater. Sci.*, **34** 3875-3882 (1999).

20. S. R. Choi and J. P. Gyekenyesi, "Load-Rate Dependency of Ultimate Tensile Strength in Ceramic Matrix Composites at Elevated Temperatures," *Int. J. Fatigue*, **27** 503-510 (2005).

21. S. R. Choi, N. P. Bansal, and M. J. Verrilli, "Delayed Failure of Ceramic Matrix Composites in Tension at Elevated Temperatures," *J. Euro. Ceram. Soc.*, **25**[9] 1629-1636 (2005).

22. (a) S. R. Choi and J. A. Salem, "Preloading Technique in Dynamic Fatigue Testing of Glass and Ceramics with an Indentation Flaw System," *J. Am. Ceram. Soc.*, **79**[5] 1228-32 (1996). (b) S. R. Choi and J. P. Gyekenyesi, "Fatigue Strength as a Function of Preloading in Dynamic Fatigue Testing of Glass and Ceramics, *ASME J. Eng. Gas Turbines and Power*, **119** 493-499 (1997).

23. C. A. Lewinsohn, C. H. Henager and R. H. Jones, "Environmentally Induced Time-Dependent Failure Mechanism in CFCCS at Elevated Temperatures," *Ceram. Eng. Sic. Proc.*, **19**[4] 11-18 (1998).

24. C. H. Henager and R. H. Jones, "Subcritical Crack Growth in CVI Silicon Carbide Reinforced with Nicalon Fibers: Experiment and Model," *J. Am. Ceram. Soc.*, **77**[9] 2381-94 (1994).

25. S. M. Spearing, F. W. Zok and A. G. Evans, "Stress Corrosion Cracking in a Unidirectional Ceramic-Matrix Composite," *J. Am. Ceram. Soc.*, **77**[2] 562-70 (1994).

26. J. A. DiCalro, "Creep and Rupture Behavior of Advanced SiC Fibers," Proc. ICCM-10, **6**, 315 (1995).

27. S. R. Choi and J. P. Gyekenyesi, "'Ultra'-Fast Fracture Strength of Advanced Structural Ceramics at Elevated Temperatures: An Approach to High-Temperature 'Inert' Strength," pp. 27-46 in *Fracture Mechanics of Ceramics*, Vol. 13, Edited by R. C. Bradt, D. Munz, M. Sakai, V. Ya. Shevchenko, and K. W. White, Kluwer Academic/Plenum Publishers, New York (2002).

THIS PAGE INTENTIONALLY LEFT BLANK

DISTRIBUTION:

Office of Naval Research, Dr. David A. Shifler, 875 N. Randolph Street Suite 1425/ONR 332, Arlington, VA 22203	(1)
National Aeronautics & Space Administration, Glenn Research Center, Dr. Narotam P. Bansal, 21000 Brookpark Road, MS106-5, Cleveland, OH 44135	(3)
NAVAIRWARCENACDIV (4.3.4.1/Choi), Bldg. 2188, Room 101A 48066 Shaw Road, Patuxent River, MD 20670	(20)
NAVAIRSYSCOM (AIR-5.1), Bldg. 304, Room 100 22541 Millstone Road, Patuxent River, MD 20670-1606	(1)
NAVAIRWARCENACDIV (4.12.4.3), Bldg. 407, Room 116 22269 Cedar Point Road, Patuxent River, MD 20670-1120	(1)
NAVTESTWINGLANT (55TW01A), Bldg. 304, Room 200 22541 Millstone Road, Patuxent River, MD 20670-1606	(1)
DTIC Suite 0944, 8725 John J. Kingman Road, Ft. Belvoir, VA 22060-6218	(1)